

# Deriving Tensile Properties of Glass Fiber Reinforced Polymers (GFRP) Using Mechanics of Composite Materials

Thomas I. Altanopoulos, Ioannis G. Raftoyiannis

Steel Structures Laboratory, School of Civil Engineering, National Technical University of Athens, Athens, Greece

Email: thaltan@hotmail.com

**How to cite this paper:** Altanopoulos, T.I. and Raftoyiannis, I.G. (2020) Deriving Tensile Properties of Glass Fiber Reinforced Polymers (GFRP) Using Mechanics of Composite Materials. *Open Journal of Composite Materials*, 10, 1-14.  
<https://doi.org/10.4236/ojcm.2020.101001>

**Received:** October 16, 2019

**Accepted:** November 29, 2019

**Published:** December 2, 2019

Copyright © 2020 by author(s) and Scientific Research Publishing Inc.

This work is licensed under the Creative Commons Attribution International License (CC BY 4.0).

<http://creativecommons.org/licenses/by/4.0/>



Open Access

## Abstract

This work addresses the tensile properties of glass fiber reinforced polymers (GFRP) and investigates the different ways of estimating them without the cost associated with experimentation. This attempt is achieved through comparison between experimental results, derived in accordance with the ASTM standards, and results obtained using the mechanics of composite materials. The experimental results are also compared to results derived from work by other researchers in order to corroborate the findings regarding the correlation of tensile properties of the GFRP material and the fiber volume fraction.

## Keywords

Glass Fiber-Reinforced Polymers (GFRP), Tensile Properties, Hand Lay-Up Method

## 1. Introduction

Glass fiber-reinforced polymers (GFRP) are widely used for many applications in civil engineering projects. Wind turbine towers, utility line poles and light standards are some examples. This broad and rapid evolution makes the utilization of these materials significant. Many researchers investigated experimentally and theoretically the behavior of such structures [1] [2] [3] [4]. In order to achieve this objective, they had to estimate the mechanical properties of the GFRP materials. The GFRP are produced using glass fibers and polyester isophthalic, orthophthalic or epoxy resins. Glass fibers have many benefits over carbon fibers in the construction of such structures. The low electrical conductivity, the significant strength against impacts, the low stress concentration in possible holes, the low cost and the less absorption of UV radiation make glass fiber po-

lymer an ideal choice for this type of structure [5].

The design of GFRP structures requires knowledge of the mechanical properties of the constituent materials. Such properties include the modulus of elasticity for both main directions of the material, the shear modulus and the Poisson ratio. Furthermore, the ultimate tensile and compressive strengths, for both main directions of the composite material, along with the in-plane shear strength, are needed. These properties are usually derived from experiments using standard coupons and tested according to acceptable procedures [6]-[11].

It may be possible, however, to estimate these properties using mechanics of composite materials. "The rule of mixture" is the theory that uses several mathematical expressions in order to obtain the required values [12]. In the present paper, these expressions are applied and the results are compared to the experimental results derived from 19 tensile tests conducted at the Steel structure Laboratory of the National Technical University of Athens (N.T.U.A), Greece. The tension coupons were fabricated using the hand lay-up method. The conclusions of the comparison are discussed thoroughly in the present paper. The utilization of these formulas demands knowledge of the fiber volume fraction of the material which is the ratio of the volume of the glass fibers to the total volume [12]. The influence of the fiber volume fraction on GFRP materials, in which polyester isophthalic resin is used as matrix, is also investigated. Particularly, experimental results are used to confirm the mathematical function that connects the fiber volume fraction and tensile properties of GFRP materials.

## 2. Experimental Investigation

### 2.1. Fabrication of Specimens

The individual materials that were used in the fabrication of the specimens included E-glass fibers and isophthalic polyester resin. The fibers were provided in the form of unidirectional fabric. The weight of the fabric was 430 g/m<sup>2</sup>. The resin used was AROPOL K530 isophthalic polyester produced by Ashland. Two panels were constructed. One panel was used for the production of coupons with fiber direction of 0° and coupons of 90°. This was achieved by placing four layers of fabric one upon the other on a glass surface. The other panel was used to make coupons of a laminate with stacking sequence ±45°. This was accomplished by placing 16 fabrics one upon the other changing the fiber direction from 0° to 90° every time. The fabrics for both cases were cut by scissors in the required dimensions (see **Figure 1(a)**). The resin reacted with its hardener and was weighed prior to use (see **Figure 1(b)**). The weight of the fibers was also known by the number of the used fabrics. Since the mass density for both fibers and resin was known by their manufacturer the fiber volume fraction of the laminate was estimated, based on the assumption that there was no void in the laminate, using the following relations:

$$v_f = V_f / V_{tot} \quad (1)$$

where,  $v_f$  is the fiber volume fraction;  $V_f$  is the volume of the fibers defined as,

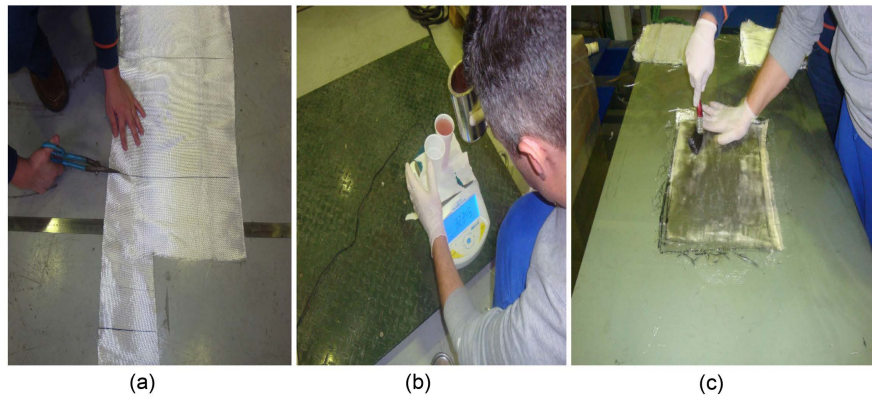


**Figure 1.** Preparation of coupons. (a) Fabric preparation; (b) Weighing of resin; (c) Panel construction with the hand lay-up method.

$$V_f = W_f / \rho_f$$

And,

$$V_{tot} = V_f + V_m \quad (2)$$

where,  $W_f$  is the weight of the fibers,  $\rho_f$  is the mass density of the fibers.

And,

$$V_m = W_m / \rho_m, \quad (3)$$

where,  $W_m$  is the weight of the matrix,  $\rho_m$  is the mass density of the matrix.

The hand lay-up method was used for the fabrication of the panels (see **Figure 1(c)**). The curing process lasted 24 hours (see **Figure 2(a)**, **Figure 2(b)**).

The dimensions of the coupons cut from the first panel were 15 mm × 250 mm for the 0° fiber direction and 24 mm × 180 mm for the 90° fiber direction, in accordance with the ASTM Standards [6], as shown in **Figure 3(a)** and **Figure 3(b)**. Their thickness was 1.6 mm. On the second panel, parallel lines at 45° were drawn in order to extract coupons with 25 mm × 200 mm dimensions, as shown in **Figure 3(c)** [7]. The average thickness of these specimens was 6 mm.

All coupons were carefully extracted from the panels, weighed and their dimensions recorded (see **Figure 4**). Accurate measurement regarding the thickness and the width of the specimens were taken in accordance with ASTM standards [6]. Particularly, measurements at three places were taken and the average cross-sectional area was recorded. A total of 19 coupons were fabricated. Seven with a fiber direction of 0°, seven with fiber direction of 90° and five with a stacking sequence of ±45° (see **Figure 5**).

## 2.2. Preparation of Coupons for Testing

According to ASTM standards [6], tabs must be used to reinforce the coupons in the area clamped by the testing machine in order to avoid being crashed. In the current experimental investigation, tabs made of emery cloth were used in the coupons with 90° fiber direction. This procedure was not followed for the coupons with ±45° fiber direction due to the fact that their significant thickness

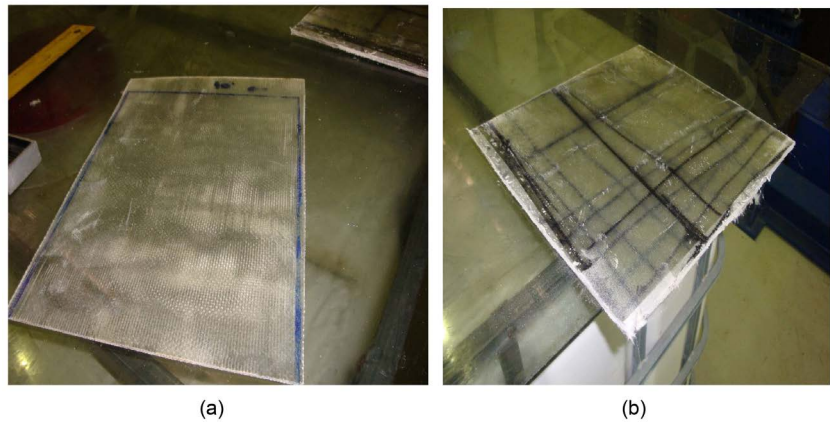


**Figure 2.** GFRP panels after curing. (a) Panel for the fabrication of coupons with fiber direction  $0^\circ$  and  $90^\circ$ ; (b) Panel after curing process for the fabrication of coupons with stacking sequence  $\pm 45^\circ$ .

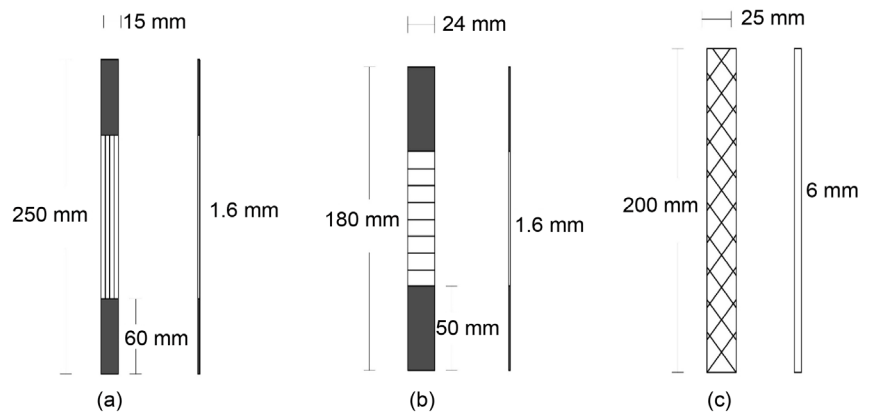


**Figure 3.** Dimensions of coupons. (a) Dimensions of coupons with  $0^\circ$  fiber direction; (b) Dimensions of coupons with  $90^\circ$  fiber direction; (c) Dimensions of coupons with  $\pm 45^\circ$  fiber orientation.

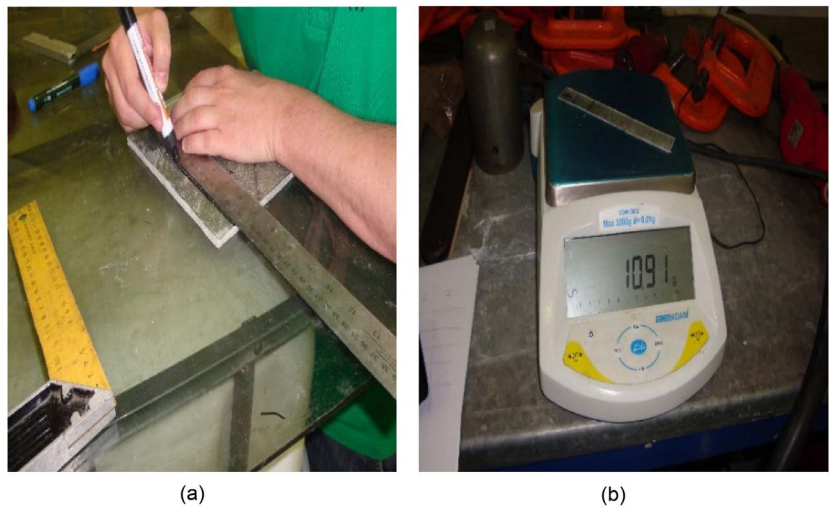


**Figure 4.** Extracting and weighing individual coupons. (a) Extracting coupons from panels; (b) Weighing of coupons.

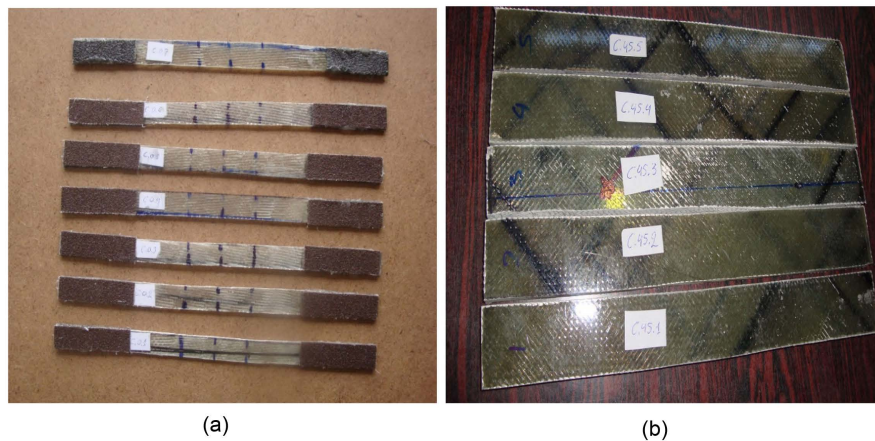


**Figure 5.** Coupons prior to testing. (a) Coupons with  $0^\circ$  fiber direction; (b) Coupons with  $\pm 45^\circ$  fiber direction.

protects them from local failure during testing. For the coupons with a fiber direction of  $0^\circ$ , tabs made of emery cloth were initially used but these failed at low tension stress at about 300 MPa. Thus, the tabs were removed letting only a slight surface of emery in contact with the grips of the testing machine just for the protection of the coupons. This problem did not occur in the coupons with  $90^\circ$  fiber direction, because the failure of the specimens occurred at a stress level significantly lower than 300 MPa. For the placement of the tabs a strong epoxy glue of two constituents was used (see **Figure 6**).

Finally, all the coupons were marked at the middle which was the point that the extensometer was placed during the tensile tests.

### 2.3. Tensile Tests

The coupons were tested at a nearly constant strain rate. Therefore, a constant head speed of a displacement rate 2 mm/min was implemented. Seven coupons with  $0^\circ$  fiber direction were tested exhibiting similar type of failure (**Figure 7**).

The failure type, according to ASTM D3039 [6], can be characterized as AGM (Angled failure type, Gage failure area, Middle failure location) (see **Figure 8**).

Seven coupons with  $90^\circ$  fiber direction laminates were also tested in the same way. All specimens exhibited similar failure type. The ultimate stress, as was anticipated, was significantly lower than the coupons with  $0^\circ$  fiber direction (**Figure 9**).

The failure type of these specimens is categorized by ASTM Standard [6] as LGM (Lateral failure type, Gage failure area, Middle failure location) (see **Figure 10**). One specimen failed at very low stress in comparison with the others. This specific coupon was excluded from the analysis of the results.

Five coupons with  $\pm 45^\circ$  fiber orientation laminates were tested. The ASTM Standard [7] provides a method of estimating the in-plane shear response of a GFRP by performing tensile tests as described in ASTM [6]. According to the composite material theory, the maximum in-plane shear stress is half of the

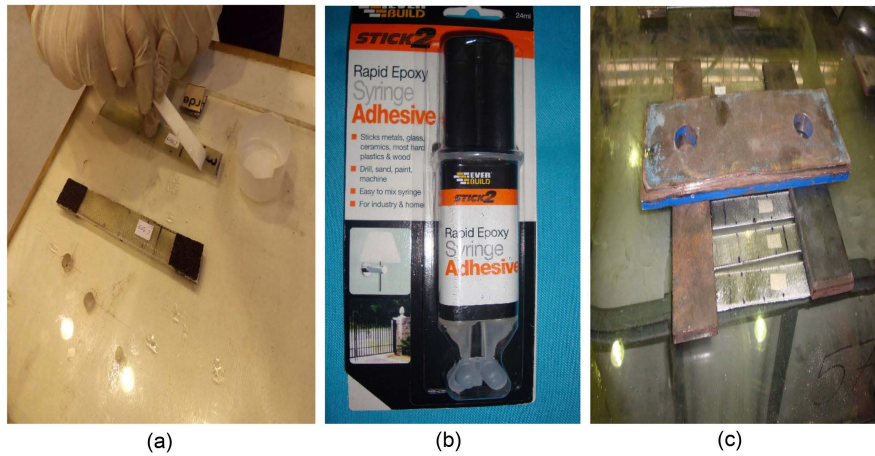


**Figure 6.** Placement of tabs. (a) Applying epoxy; (b) Epoxy glue used for the placement of the tabs; (c) Applying weight to ensure uniform spreading of epoxy.

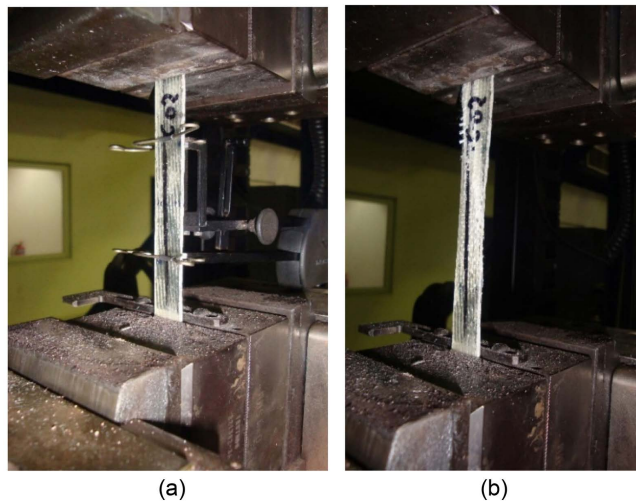


**Figure 7.** Coupon with 0° fiber orientation before and after testing. (a) Coupon before testing; (b) Coupon after testing.



**Figure 8.** Characteristic failure type of coupons with 0° fiber orientation.

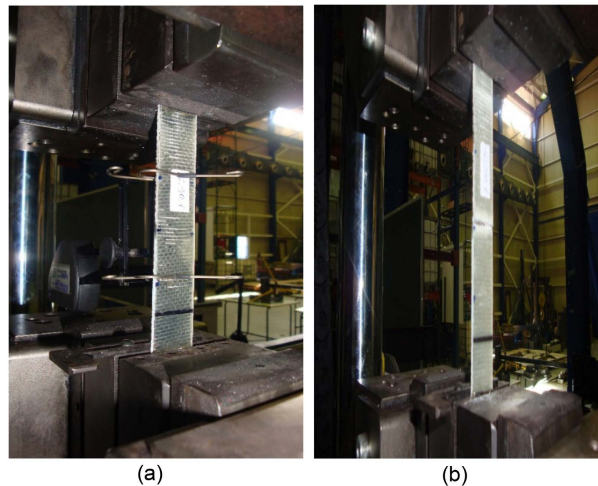


**Figure 9.** Coupon with 90° fiber direction before and after tensile test. (a) Coupon prior to testing; (b) Coupon after testing.



**Figure 10.** Characteristic failure type of coupons with 90° fiber orientation.

maximum normal tensile stress for a symmetrical laminate with a  $\pm 45^\circ$  stacking sequence [7].

$$\tau_{12} = \sigma_x / 2 \quad (4)$$

It should be mentioned, however, that due to fiber scissoring during tension the ultimate tensile strength to be used in Equation (4) is the one that occurs in the range of 5% shear strain [7]. In order to estimate the shear strain during the tensile test, strain gages in both longitudinal and transverse directions must be used. In that case,

$$\gamma_{12} = \varepsilon_x - \varepsilon_y \quad (5)$$

This was not feasible at this testing process (Figure 11).

The failure type of these coupons can be characterized as DGV (Edge delamination with almost simultaneously angled failure type, Gage failure area in most cases, Various failure location) (see Figure 12).

## 2.4. Tests Results

The test results of coupons with 0° fiber orientation are shown in Figure 13 and

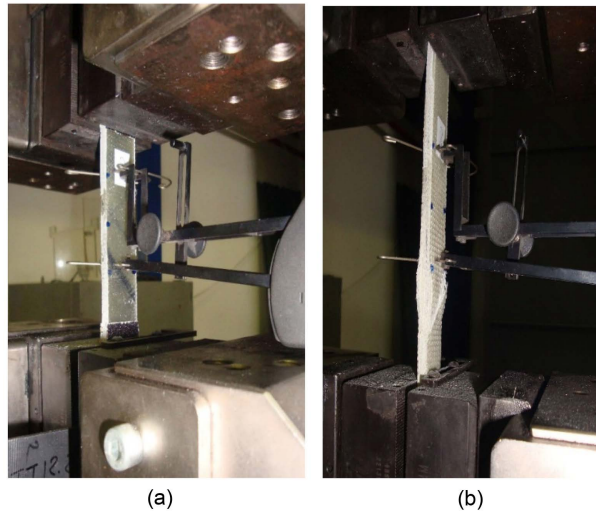


**Figure 11.** Coupon with  $\pm 45^\circ$  fiber orientation before and after testing. (a) Coupon prior to testing; (b) Coupon after testing.

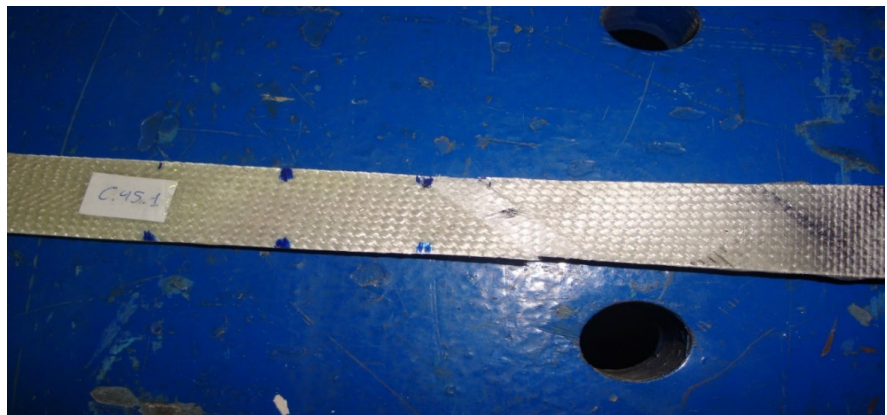


**Figure 12.** Characteristic failure type of a coupon with  $\pm 45^\circ$  fiber orientation.

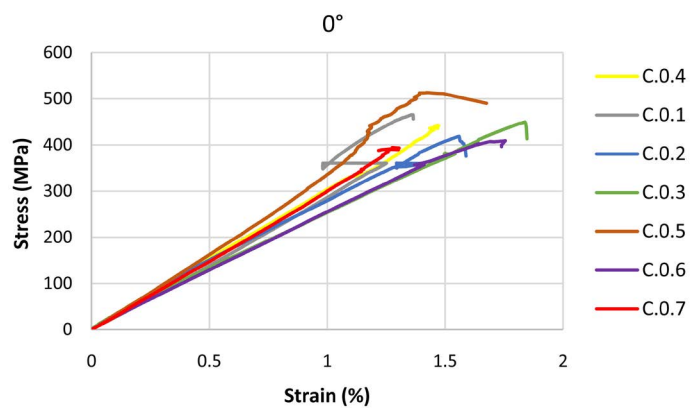


**Figure 13.** Stress-strain behavior of coupons with  $0^\circ$  fiber orientation.

are listed in **Table 1**. The mean ultimate tensile strength was 441.64 MPa. The extensometer was removed from the coupon C.0.1 at, approximately, a 75% of the ultimate load to prevent damage. However, load recording was continued

**Table 1.** Test results of coupons with 0° fiber orientation.

Coupons	Max Stress (MPa)	Mean Stress (MPa)	CV (%)	E <sub>1</sub> (MPa)	Mean E <sub>1</sub> (MPa)	CV (%)
C.0.1	465.32			27,436.81		
C.0.2	418.40			31,109.26		
C.0.3	449.34			26,668.47		
C.0.4	441.98	441.64	9.04	30,677.48	29,046.27	8.75
C.0.5	513.10			31,967.24		
C.0.6	408.96			25,319.50		
C.0.7	394.36			30,145.13		

until a complete failure was observed. The tensile modulus of elasticity was calculated according the ASTM Standard [6]. The stress values at the strain point of 0.1% and 0.3% were used for estimating the modulus of elasticity of each specimen. There was no transition region (defined as a significant change in the slope of the stress-strain curve) within this strain range. The mean value of the tensile modulus of elasticity was calculated to be 29.05 GPa.

The test results of the coupons with 90° fiber direction are shown in **Figure 14** and are listed in **Table 2**. The mean ultimate tensile stress was 56.56 MPa. The modulus of elasticity was initially calculated at the same strain range as that of the coupons with 0° fiber orientation (0.1% - 0.3%). Since some specimens presented a change in slope (transition region) in the stress-strain curve around 0.3% strain another range was chosen to determine the modulus of elasticity. The range chosen was between 0.1% and 0.25% strain. The mean value of the tensile modulus of elasticity perpendicular to the fiber direction was 6.33 GPa.

The test results of the coupons with ±45° fiber orientation are shown in **Figure 15** and are listed in **Table 3**. The mean ultimate tensile stress was 90.66 MPa. According to the mechanics of composite materials the in-plane shear strength of the particular composite material may be obtained from Equation (4) to be  $90.66/2 = 45.33$  MPa [7]. As discussed in Section 2.3, this could be the case if the tensile failure occurs in the range of 5% shear strain. However, as shown in **Figure 15**, failure occurred at tensile strains above 7%. In this study, the shear stress at strain 3.33% tensile strain was obtained. Assuming a plastic condition with a Poisson ratio of 0.5 and using Equation (5), the tensile strain value of 3.33% seems a satisfactory approach. Thus, an estimation for the in-plane shear strength, using Equation (4), is  $70.97/2 = 35.49$  MPa.

### 3. Discussion of Results

The tensile modulus of elasticity for both main directions of the composite material, along with the Poisson ratio and the shear modulus, can be calculated using the “rules of mixture” [12]. The modulus of elasticity in the direction of the fibers may be derived as follows:

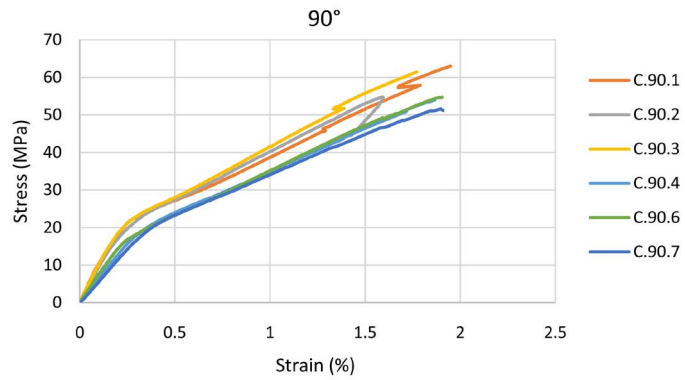


Figure 14. Stress-strain behavior of coupons with 90° fiber orientation.

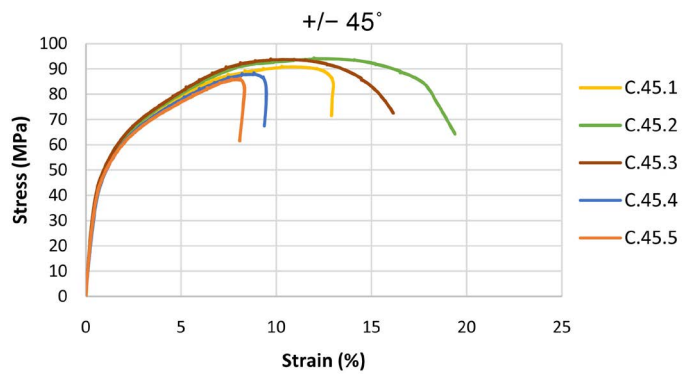


Figure 15. Stress-strain behavior of coupons with ±45° fiber orientation.

Table 2. Test results of coupons with 90° fiber orientation.

Coupons	Max Stress (MPa)	Mean Stress (MPa)	CV (%)	E <sub>2</sub> (MPa)	Mean E <sub>2</sub> (MPa)	CV (%)
C.90.1	62.96			7042.46		
C.90.2	54.73			6293.44		
C.90.3	61.42			6784.73		
C.90.4	53.94	56.56	8.01	6037.57	6327.33	7.85
C.90.6	54.66			6085.44		
C.90.7	51.63			5720.39		
C.90.5 X	21.00					

Table 3. Test results of coupons with ±45° fiber orientation.

Coupons	Max Stress (MPa)	Mean Stress (MPa)	CV (%)	Stress at 3.33% (MPa)	Mean Stress (MPa)	Estimated Shear Strength (MPa)
C.45.1	91.01			70.88		
C.45.2	94.33			71.84		
C.45.3	93.72	90.66	3.95	72.65	70.97	35.49
C.45.4	88.43			70.01		
C.45.5	85.82			69.49		

$$E_1 = E_f v_f + E_m v_m \quad (6)$$

where,  $E_f$  and  $E_m$  are the moduli of elasticity for fibers and matrix, respectively;  $v_f$  is the fiber volume fraction; and  $v_m$  is the matrix volume fraction. The fiber volume fraction for the tested material was determined, during the manufacturing of the composite panels, using the weight of the materials. After the extraction of the coupons, every coupon was weighed, and its dimensions (length, thickness and width) were recorded. Given the number of the fabrics, four, and their weight, the total weight and volume of the fibers in each coupon was determined, since their mass density was provided by the manufacturer. Thus, the fiber volume fraction was estimated for each coupon. The mean value of the fiber volume fraction was 41%. The values for  $E_f$  and  $E_m$  are 72,000 MPa and 4100 MPa, respectively, as provided by the manufacturer. The matrix volume fraction,  $v_m$ , was obtained by neglecting the volume of the void inside the material. This is acceptable due to the fact that the particular composite material was constructed using the hand lay-up method. Thus,

$$v_m = 1 - v_f = 0.59 \quad (7)$$

Substituting the above values to Equation (6),

$$E_1 = 72000 \times 0.41 + 4100 \times 0.59 = 31939 \text{ MPa} .$$

According to the “rules of mixture” the transverse tensile modulus of elasticity is:

$$E_2 = (E_f E_m) / (v_m E_f + v_f E_m) \quad (8)$$

For the known parameters,

$$E_2 = (72000 \times 4100) / (0.59 \times 72000 + 0.41 \times 4100) = 6684.63 \text{ MPa} .$$

The moduli of elasticity calculated on the basis of the information provided by the manufacturer are compared to those obtained experimentally in **Table 4**. The average values for longitudinal and transverse moduli of elasticity are listed. As shown in **Table 4**, the theoretical results are very close to the experimental ones. Thus, the mechanics of composite materials can be used in order to obtain the mechanical properties that are required for the design of GFRP structures.

The results obtained in this research investigation were also compared to results obtained by other researchers. More specifically the comparison focused on the tensile strength and the modulus of elasticity of GFRP manufactured, using as matrix an isophthalic resin, as a function of the fiber volume fraction. In the papers referenced in **Table 5**, experimental data were derived using the ASTM Standard [6], as was also the case in the present work. The results are plotted in **Figure 16** and **Figure 17**. As shown in these figures, the fiber volume fraction affects significantly both the tensile strength and the tensile modulus of elasticity in the fiber direction of the composite material. An increase in  $v_f$  causes a proportional enhancement to the mechanical properties. The relationship between these properties and  $v_f$  appears to be linear as described by the theoretical expression (Equation (6)), presented in Section 3. Any deviation from a perfectly

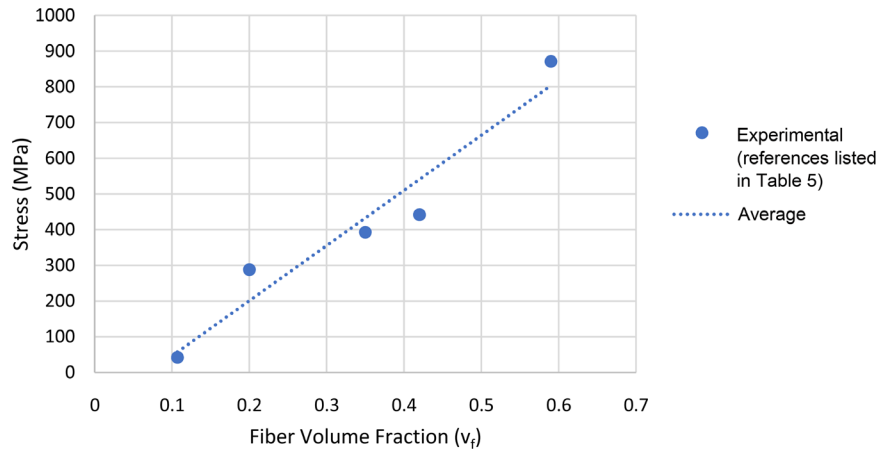


**Figure 16.** Tensile strength of coupons with fibers in the 0° direction as a function of fiber volume fraction,  $v_f$ .

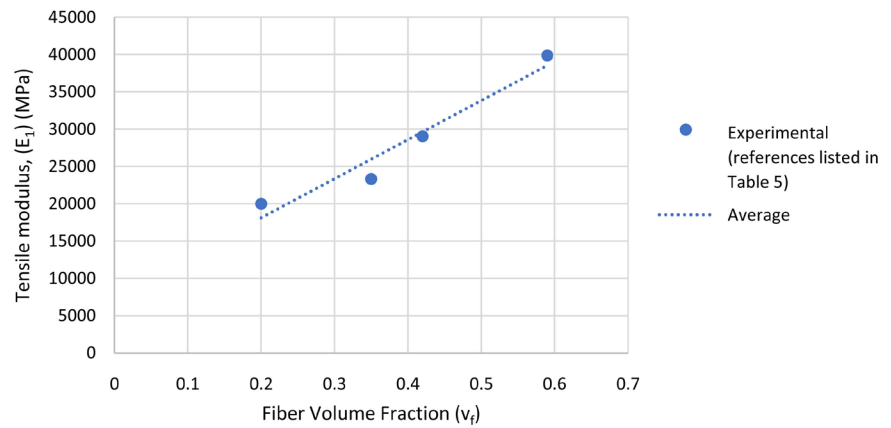


**Figure 17.** Tensile modulus of elasticity as a function of fiber volume fraction,  $v_f$ .

**Table 4.** Tensile modulus of elasticity (MPa).

Tensile Modulus of Elasticity (MPa)	Experimental Results	Theoretical Values	Theoretical/Experimental
In the fiber direction ( $E_1$ )	29,046.27	31,939.00	1.09
Perpendicular to the fiber direction ( $E_2$ )	6327.33	6684.63	1.06

**Table 5.** Values of ultimate tensile stress and modulus of elasticity for different fiber volume fraction.

References	Fiber volume fraction $v_f$	Tensile strength in coupons with fibers in 0° direction(MPa)	Tensile modulus of elasticity (MPa)
[9]	0.107	42.00	-
[8]	0.2	288.00	20,000
[10]	0.35	392.72	23,320
Present study	0.42	441.64	29,046
[11]	0.59	871.00	39,887

linear response could be attributed to the fact that the matrix of the tested materials is not always the same isophthalic polyester resin. Furthermore, the glass fibers are not of the same type. For instance, in the present study the fibers are in the form of a unidirectional fabric. In other experiments, chopped fibers are used. The tensile strength of fibers varies and, therefore, the mechanical properties of the produced GFRP could be affected.

#### 4. Conclusions

The key objective of this research program was to investigate the different ways of estimating the tensile properties of GFRP without the cost associated with experimentation. This objective was achieved through comparison between experimental results, derived from coupon testing, in accordance with the ASTM standards, and results obtained using the mechanics of composite materials. The experimental results are also compared in this paper to results derived from work by other researchers in order to corroborate the findings regarding the correlation of tensile properties of the GFRP material and the fiber volume fraction. The key findings from this work are:

- Mechanics of composite materials offer an excellent approach for the calculation of the GFRP properties, such as Modulus of elasticity and Ultimate tensile strength. However, information regarding the properties of resin and the fibers provided by the manufacturers should be reliable.
- The fiber volume fraction plays a major role in the mechanical properties of a GFRP. The linear correlation between  $v_f$  and these properties is consistent with the principles of the “rules of mixture”.

#### Acknowledgements

The first author, Thomas Altanopoulos expresses his gratitude to the staff of the Steel Structures Laboratory of the National Technical University of Athens for their assistance in conducting the experimental work. In addition, he acknowledges, with deep sorrow, the unexpected passing of the second author, the late Dr. Ioannis Raftoyiannis, whose distinguished contribution to the field and exceptional mentorship made this project possible. Finally, the first author would like to thank Dr. Dimos Polyzois, Professor Emeritus at the University of Manitoba, Canada, who graciously agreed to step in as supervisor following the passing of Dr. Raftoyiannis.

#### Conflicts of Interest

The authors declare no conflicts of interest regarding the publication of this paper.

#### References

- [1] Polyzois, D., Raftoyiannis, I.G. and Philopoulos, D. (2007) An Experimental Survey of the Static and Dynamic Behavior of Jointed Composite GFRP Tapered Poles. *Mechanics of Advanced Materials and Structures*, **14**, 203-212.

- <https://doi.org/10.1080/15376490600734849>
- [2] Gay, D., Hoa, S.V. and Tsai, S.W. (2003) Composite Materials Design and Application. CRC Press LLC, London. <https://doi.org/10.1201/9781420031683>
  - [3] Polyzois, D.J., Raftoyiannis, I.G. and Ungkurapinan, N. (2009) Static and Dynamic Characteristics of Multi-Cell Jointed GFRP wind Turbine Towers. *Composite Structures*, **90**, 34-42. <https://doi.org/10.1016/j.compstruct.2009.01.005>
  - [4] Raftoyiannis, I.G. and Polyzois, D.J. (2007) The Effect of Semi-Rigid Connections on the Dynamic Behavior of Tapered Composite GFRP Poles. *Composite Structures*, **81**, 70-79. <https://doi.org/10.1016/j.compstruct.2006.07.015>
  - [5] ASCE FRP Task Committee (2016) Pre-Standard for Utility Line Poles Made of FRP, Chapter Combined Edited.
  - [6] ASTM D3039/D3039M-00 (2000) Standard Test Method for Tensile Properties of Polymer Matrix Composite Materials. ASTM International, West Conshohocken, PA.
  - [7] ASTM D3518/D3518M-94 (2001) Standard Test Method for in-Plane Shear Response of Polymer Matrix Composite Materials by Tensile Test of a  $\pm 45^\circ$  Laminate. ASTM International, West Conshohocken, PA.
  - [8] Horlle de Oliveira, F., Helfer, A.L. and Amico, S.C. (2012) Mechanical Behavior of Unidirectional Curaua Fiber and Glass Fiber Composites. *Macromolecular Symposia*, **319**, 83-92. <https://doi.org/10.1002/masy.201100202>
  - [9] Gupta, G., Gupta, A., Dhanola, A. and Raturi, A. (2016) Mechanical Behavior of Glass Fiber Polyester Hybrid Composite Filled with Natural Fillers. *IOP Conference Series: Materials Science and Engineering*, **149**, Article ID: 012091. <https://doi.org/10.1088/1757-899X/149/1/012091>
  - [10] Smith, K.J. (2005) Compression Creep of a Pultruded-Glass/Polyester composite at Elevated Service Temperatures. Master of Science Thesis, Georgia Institute of Technology, Atlanta, GA.
  - [11] Bramante, G., Bertucelli, L., Benvenuti, A. and Meyer, K.J. (2014) Polyurethane Composites: A Versatile Thermo-Set Polymer Matrix for Abroad Range of Applications. *Polyurethanes 2014, Polyurethanes Technical Conference*, Dallas, TX, 22-24 September 2014, 507-522.
  - [12] Kollar, L.P. and Springer, G.S. (2003) Mechanics of Composite Structures. Cambridge University Press, Cambridge.